

Decay of a  $\pi h_{11/2} \otimes \nu h_{11/2}$  microsecond isomer in  $^{136}\text{Pm}_{75}$ 

S. V. Rigby,<sup>1</sup> D. M. Cullen,<sup>1</sup> P. J. R. Mason,<sup>1</sup> D. T. Scholes,<sup>1</sup> C. Scholey,<sup>2</sup> P. Rahkila,<sup>2</sup> S. Eeckhaudt,<sup>2</sup> T. Grahn,<sup>2,\*</sup> P. Greenlees,<sup>2</sup> P. M. Jones,<sup>2</sup> R. Julin,<sup>2</sup> S. Juutinen,<sup>2</sup> H. Kettunen,<sup>2</sup> M. Leino,<sup>2</sup> A.-P. Leppänen,<sup>2</sup> P. Nieminen,<sup>2,†</sup> M. Nyman,<sup>2</sup> J. Pakarinen,<sup>2,\*</sup> and J. Uusitalo<sup>2</sup>

<sup>1</sup>Schuster Laboratory, School of Physics and Astronomy, University of Manchester, Manchester, M13 9PL, United Kingdom

<sup>2</sup>Department of Physics, University of Jyväskylä, Jyväskylä, FIN-40014, Finland

(Received 8 May 2007; revised manuscript received 18 April 2008; published 3 September 2008)

An experiment has been performed to populate several extremely neutron-deficient nuclei around the mass-140 region of the nuclear chart, using a beam of  $^{54}\text{Fe}$  on a  $^{92}\text{Mo}$  target at an energy of 315 MeV. Analysis of these data using recoil-isomer tagging has established that the yrast  $\pi h_{11/2} \otimes \nu h_{11/2}$ ,  $J^\pi = (8^+)$ , bandhead state in  $^{136}\text{Pm}$  is isomeric with a half-life of 1.5(1)  $\mu\text{s}$ . This isomeric state decays via a 43-keV, probable- $E1$  transition to a  $J^\pi = (7^-)$  state. Consideration of the theoretical Nilsson orbitals near the Fermi surface suggests that the  $J^\pi = (8^+)$  state has a  $\nu h_{11/2}[505]_{1/2}^- \otimes \pi h_{11/2}[532]_{3/2}^-$  configuration, which decays to the  $J^\pi = (7^-)$  state with a  $\nu h_{11/2}[505]_{1/2}^- \otimes \pi d_{5/2}[411]_{3/2}^+$  configuration. Differences in the shape-driving effects for these two configurations is reasoned to be responsible for the long half-life of the  $J^\pi = (8^+)$  isomeric state. The non-observation of other  $\gamma$  rays in prompt or delayed coincidence with the 43-keV transition suggests that this transition may feed another, longer lived isomeric state with a half-life of the order of milliseconds or greater. However, the present experiment was not sensitive to the decay of this new  $J^\pi = (7^-)$  state by internal conversion or even  $\beta$  decay.

DOI: 10.1103/PhysRevC.78.034304

PACS number(s): 23.20.Lv, 21.10.Tg, 27.60.+j

## I. INTRODUCTION

Neutron-deficient nuclei around mass  $A = 130$ – $140$  are known to be  $\gamma$  soft [1–4]. Their shapes are influenced by quasiparticles in high- $j$  orbitals. The proton configuration favors a prolate shape with  $\gamma = 0^\circ$ , since it involves a small number of particles in the high- $j$   $h_{11/2}$  orbit; whereas the neutron configuration favors an oblate shape with  $\gamma = 60^\circ$ , since it includes a small number of holes in the  $h_{11/2}$  neutron shell [2]. Competition between the shape-driving effects of the proton and neutron orbits often results in triaxial shapes in these nuclei. Variations in shapes between different structures within the nucleus can result in isomeric states as the transitions between these states are hindered. Several microsecond isomeric states resulting from such competition have been observed in the  $N = 77$  nuclei  $^{140}\text{Eu}$ ,  $^{142}\text{Tb}$ , and  $^{144}\text{Ho}$  [5,6].

The neighboring  $N = 75$ , doubly odd nucleus,  $^{136}\text{Pm}$ , has been the subject of several high-spin studies [3,4,7–10]. These studies established that the yrast band is based upon a  $\pi h_{11/2} \otimes \nu h_{11/2}$ ,  $J^\pi = (8^+)$  configuration [3,7]. Although this assignment is tentative, it fits the systematics of spins assigned to  $\pi h_{11/2} \otimes \nu h_{11/2}$  configurations in this region. In addition, several side bands have been observed in  $^{136}\text{Pm}$ , including a band built upon the  $\nu h_{11/2} \otimes \pi g_{7/2}$  configuration [3], which becomes yrast at high spin.  $\gamma$ -soft triaxial nuclear states are, among others, well established in  $^{136}\text{Pm}$ , and evidence has even

been presented for its chiral behavior [4,10]. The low-spin states of  $^{136}\text{Pm}$  have been studied in  $\beta$  decay, where two long-lived, low-lying states were established [11]: a  $J^\pi = (5^-)$  state with a half-life of 1.8 min, which is thought to be the ground state, and a  $J^\pi = (2^+)$  state with a half-life of 47 s, which is thought to be a low-lying isomeric state. The order of these two states in excitation energy remains ambiguous. To date, nothing is known about how the  $\pi h_{11/2} \otimes \nu h_{11/2}$ ,  $J^\pi = (8^+)$  state is connected to these lower-lying states, and consequently the excitation energy of this state has not yet been determined.

This paper reports the observation of a 1.5(1)  $\mu\text{s}$  isomer in  $^{136}\text{Pm}$  which is assigned to the known yrast  $J^\pi = (8^+)$  bandhead state. The isomer subsequently decays to a  $J^\pi = (7^-)$  state via a 43-keV  $\gamma$  ray whose reduced-transition strength is consistent with  $E1$  multipolarity and the systematics of isomeric decays in the neighboring nuclei. The long lifetime of the isomeric state is reasoned to be due to the differing shape-driving effects of the  $J^\pi = (8^+)$  and  $J^\pi = (7^-)$  configurations. In the present work, no prompt or delayed  $\gamma$ -ray coincidences were found to link the new  $J^\pi = (7^-)$  state to the lower-spin long-lived  $J^\pi = (5^-)$  and  $(2^+)$  states observed in the  $\beta$ -decay work [11]. This may suggest that the newly observed  $J^\pi = (7^-)$  state may feed another, longer-lived, isomeric state with a half-life of the order of milliseconds or greater, or that this longer-lived state does not decay by emission of  $\gamma$  rays, but by  $\beta$  decay or internal conversion.

## II. EXPERIMENT

$^{136}\text{Pm}$  nuclei were produced, along with a variety of other nuclei from this region, using a heavy-ion fusion-evaporation

\*Present address: Oliver Lodge Laboratory, University of Liverpool, Liverpool, L69 3BX, United Kingdom.

†Present address: Department of Nuclear Physics, Research School of Physical Sciences and Engineering, Australian National University, Canberra, ACT 0200, Australia.

reaction. The K130 cyclotron in Jyväskylä, Finland, was used to accelerate a beam of  $^{54}\text{Fe}$  onto a  $500\text{-}\mu\text{g}/\text{cm}^2$   $^{92}\text{Mo}$  target, at an energy of 315 MeV, forming the compound nucleus  $^{146}\text{Er}$ . The prompt  $\gamma$  rays were recorded with the JUROGAM high-purity (HP) Ge detector array, which consists of a total of 43 HPGe detectors, each with a bismuth germanate (BGO) anti-Compton shield. The recoiling nuclei passed through the gas-filled separator recoil ion transport unit (RITU) [12] and into the GREAT focal plane spectrometer [13]. The GREAT focal plane array consisted of a multiwire proportional counter (MWPC), an array of pin diodes, two double-sided silicon strip detectors (DSSDs) and a segmented planar-Ge detector. The recoiling nuclei passed through the MWPC, where energy loss was recorded, and were implanted into the silicon detectors, where the positions of the recoils were measured.  $\gamma$  rays from the deexcitation of isomeric states in the implanted nuclei were subsequently detected in the planar-Ge detector. A two-dimensional gate was applied in the software [14] during the offline sorting, using the energy loss from the recoils recorded in the MWPC and the time of flight recorded between the MWPC and the DSSDs, to distinguish recoiling nuclei from any transported or scattered beam. This condition ensured that only events from the evaporation residues were used in the final analysis. The average beam current was  $\approx 6$  pA, which produced a total prompt  $\gamma$ -ray rate of  $\approx 200$  kHz in the JUROGAM detectors and 2.4 kHz in the Si detectors at the focal plane of the RITU. The GREAT triggerless data acquisition system, total data readout (TDR) [15], was used. All the data were recorded and associated with a time-stamp generated by a 100-MHz clock.

Two-dimensional spectra (matrices) were constructed from these data using the GRAIN software package [14]. The energies of the prompt JUROGAM  $\gamma$  rays were correlated with the energies of the delayed  $\gamma$  rays from the planar detector, within 1-, 3-, 7-, and 20- $\mu\text{s}$  time intervals between the arrival of a recoil at the focal plane and the emission of a delayed  $\gamma$  ray.

This method, known as recoil-isomer tagging (RIT), was first used at Jyväskylä to successfully identify the prompt  $K^\pi = 8^-$  band in  $^{138}\text{Gd}$  [16]. These correlated matrices were analyzed using the UPAK software package [17].

### III. RESULTS

In the analysis of these data, the main prompt exit channels observed at the JUROGAM target array were  $^{140}\text{Gd}$  ( $4p2n$ , 28.2%) and  $^{139}\text{Eu}$  ( $5p2n$ , 24.1%). Other channels observed included  $^{136}\text{Sm}$  ( $\alpha 4p2n$ , 11.5%),  $^{137}\text{Sm}$  ( $\alpha 4pn$ , 10.2%), and  $^{139}\text{Gd}$  ( $5p2n$ , 9.56%). However, at the focal plane of the RITU, the most populated delayed channel observed from the  $\gamma$ -ray decay of isomeric states was  $^{140}\text{Eu}$  ( $5pn$ ). The delayed  $^{140}\text{Eu}$  photopeaks account for 4.8% of the total projection observed in the GREAT planar detector, recorded within 3  $\mu\text{s}$  after the arrival of a recoiling nucleus in the focal plane MWPC. The total projections from a 0–3  $\mu\text{s}$  RIT matrix are shown in Fig. 1; spectrum (a) shows the delayed total projection from the planar detector, with the known transitions marked (see caption for details) and Fig. 1(b) shows the prompt total projection from the JUROGAM detectors.

In this work, utilizing the RIT method to study the correlated matrices, the yrast  $\pi h_{11/2} \otimes \nu h_{11/2}$  bandhead in  $^{136}\text{Pm}$  has been established to be isomeric. Figure 2(a) shows the result of gating on a new delayed 43-keV  $\gamma$ -ray transition observed at the focal plane of the RITU [see Fig. 1(a)], in a prompt-delayed analysis with a 0–3  $\mu\text{s}$  correlation time. The resulting correlated prompt spectrum shows the established yrast band [3], along with several transitions from a known sideband in  $^{136}\text{Pm}$ . Conversely, gating on the strongest of these prompt yrast transitions and summing the gates together clearly shows the delayed 43-keV  $\gamma$  ray, see Fig. 2(b). Note that although this  $\gamma$ -ray energy is very close to the  $K_\beta$  x-ray

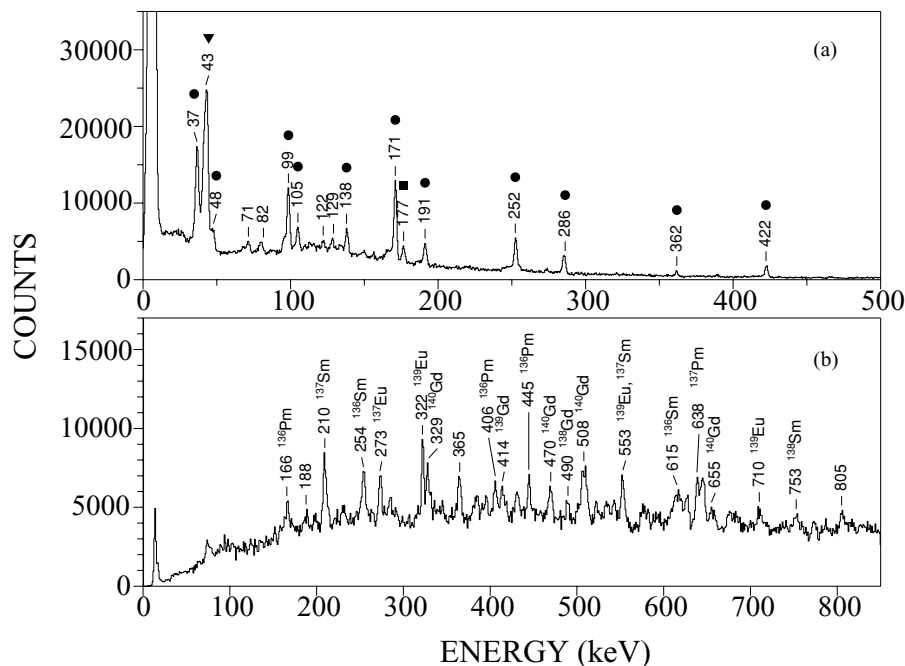


FIG. 1. (a) Delayed total projection of the GREAT planar detector taken from the 0–3  $\mu\text{s}$  prompt-delayed correlated matrix at 315 MeV. The known  $\gamma$  rays are marked: circles ( $\bullet$ ) denote  $^{140}\text{Eu}$  transitions [5] and squares ( $\blacksquare$ ) the known  $^{133}\text{Nd}$  transitions [18]. The delayed 43-keV transition assigned to  $^{136}\text{Pm}$  in this work is marked with a triangle ( $\blacktriangledown$ ). (b) Prompt total projection of the JUROGAM detectors taken from the same matrix, with the main peaks labeled.

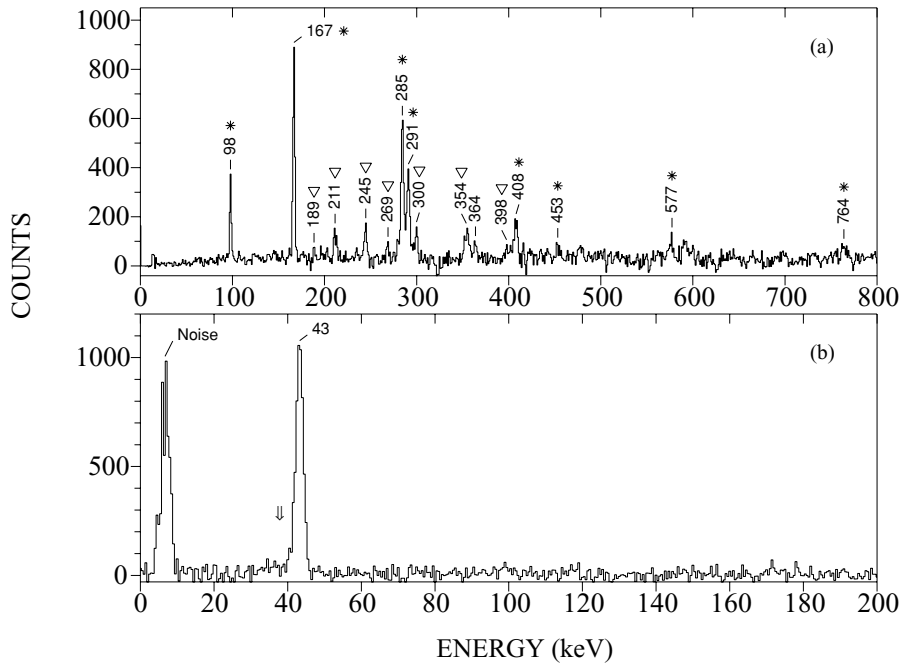


FIG. 2. (a) Result of gating on the new 43-keV delayed transition in the delayed data and projecting out the prompt  $\gamma$  rays in the 0–3  $\mu$ s prompt-delayed correlation matrix. The known yrast  $\pi h_{11/2} \otimes \nu h_{11/2}$  band in  $^{136}\text{Pm}$  is marked with asterisks (\*) and the  $\pi[413]_{2}^{5+} \otimes \nu h_{11/2}$  sideband is denoted by open triangles ( $\nabla$ ) [3]. (b) Delayed spectrum resulting from a sum of gates placed on the prompt  $^{136}\text{Pm}$  yrast transitions (98, 167, 285, 291, 408, 453, and 577 keV) in the same matrix. The newly established 43-keV delayed  $\gamma$  ray is clearly observed. The arrow indicates the position where the Pm  $K_{\alpha}$  x rays at 38.6 keV would be expected if the 43-keV transition were a  $K_{\beta}$  x ray.

energy of Pm (43.8 keV), it was not associated with the  $K_{\beta}$  x ray because the  $K_{\alpha}$  x ray would be expected to be seen in Fig. 2(b) at an energy of 38.6 keV at an even greater intensity. The nonobservation of an x-ray transition at 38.6 keV shows that this 43-keV transition is indeed a delayed  $\gamma$ -ray in  $^{136}\text{Pm}$ .

Figure 3 shows a typical half-life plot associated with the  $\gamma$ -ray emission of the delayed 43-keV transition. The time spectrum shows the time difference between a recoil implant at the focal plane and the emission of a delayed  $\gamma$  ray. A nonlinear weighted least-squares fit to the data of the form  $N = A + N_0 \exp(-\lambda t)$  is also shown, where  $N$  is the number of counts at time  $t$ ,  $A$  is the background count level,  $\lambda$  is

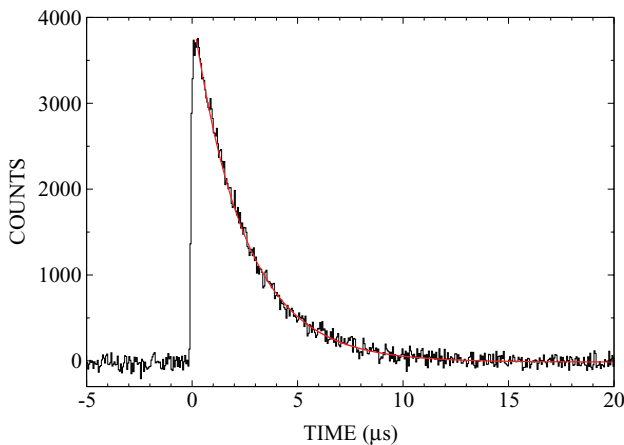


FIG. 3. (Color online) Typical spectrum showing the time difference between a recoil implant in the MWPC and the detection of the delayed 43-keV  $\gamma$ -ray transition at the focal plane. The weighted least squares fit from a series of these spectra is shown by the solid line, which represents a mean half-life of 1.5(1)  $\mu$ s.

the decay constant, and  $N_0$  is the number of counts at time  $t = 0$ . Several similar spectra were created by setting differing gates and backgrounds on the 43-keV  $\gamma$  ray. The mean and variance of these fits established the half-life of the known yrast  $J^{\pi} = (8^{+})$  bandhead state to be 1.5(1)  $\mu$ s.

A partial level scheme with energies and intensities taken from this study is shown in Fig. 4. The statistics in the present experiment did not permit the examination of recoil-isomer tagged prompt  $\gamma$ - $\gamma$  coincidence relationships or angular correlation information. Therefore the ordering of the prompt  $\gamma$ -rays above the isomer was taken from Ref. [3]. A summary of the energy and intensities of the  $\gamma$ -ray transitions assigned to  $^{136}\text{Pm}$  observed in this study is given in Table I.

Figure 4 also shows a lower-lying ( $5^{-}$ ) state observed in  $^{136}\text{Pm}$  from  $\beta$ -decay studies [11]. This state lies 27 keV below the newly observed ( $7^{-}$ ) state populated from the 43-keV  $\gamma$  decay of the isomer. The fact that the 43-keV  $\gamma$  ray is observed alone [see Fig. 2(b)] and not in coincidence with any other delayed  $\gamma$  rays (e.g., a 27-keV  $E2$  transition) suggests that the subsequent decay might feed another longer-lived isomeric state. As the 43-keV transition carries a large intensity, the nonobservation of any other transitions leads to the assumption that no other  $\gamma$  rays are populated promptly with respect to this transition. Searches were carried out for any delayed  $\gamma$  rays arriving in the planar detector following a 43-keV  $\gamma$  ray. The data implantation rate in the planar detector was approximately 100 Hz, hence the upper limit of the clean recoil- $\gamma$  gates was  $\approx 1$  ms. (The expected lifetime of a 27-keV  $E2$  transition including the conversion component is 1.64  $\mu$ s.) No  $\gamma$  rays were observed following a 43-keV  $\gamma$  ray within this time limit. This could be because the state populated by the 43-keV  $\gamma$  ray is a long-lived isomeric state, with a half-life in excess of 1 ms, as the decay from such a state would not be observed in this study. Alternatively, the state populated by the 43-keV  $\gamma$  ray

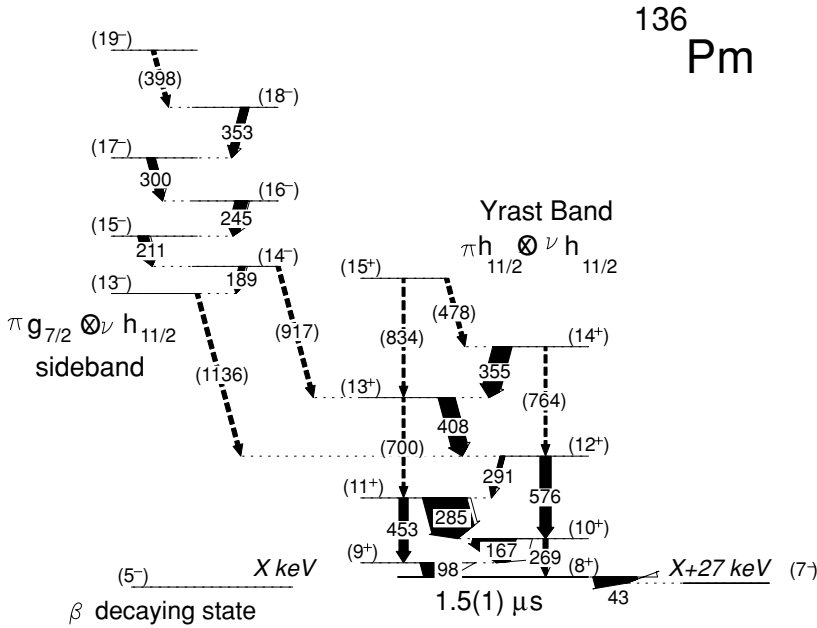


FIG. 4. Partial level scheme for  $^{136}\text{Pm}$ , showing the feeding and decay of the newly established  $1.5(1) \mu\text{s}$  ( $8^+$ ) isomer. The ordering of the prompt  $\gamma$  rays above the new isomer was taken from Ref. [3], and the lower-lying ( $5^-$ )  $\beta$ -decaying state is from Ref. [11]. The widths of the  $\gamma$ -ray transitions are proportional to their intensities with the white part representing the calculated proportion of internal conversion.

may decay via  $\beta$  decay or electron conversion, not emitting  $\gamma$  rays. Our present experiment was not sensitive to these latter two processes.

TABLE I. Energies and intensities of the  $\gamma$ -ray transitions assigned to  $^{136}\text{Pm}$  observed in this study from a 0–3  $\mu\text{s}$  prompt-delayed matrix. Intensities for the prompt transitions were fitted in a spectrum gated on the delayed 43- $\mu\text{s}$  transition and normalized to the 285-keV transition. The spins and parities of the prompt states are taken from Ref. [3].

$E_\gamma$ (keV)	$I_\gamma$	$I_i^\pi \rightarrow I_f^\pi$
Delayed $\gamma$ ray:		
42.7(2)	3.0(3)% <sup>a</sup>	( $8^+$ ) $\rightarrow$ ( $7^-$ )
Prompt $\gamma$ rays:		
$\pi h_{11/2} \otimes \nu h_{11/2}$ band:		
97.9(1)	45.6(4.9)	( $9^+$ ) $\rightarrow$ ( $8^+$ )
166.8(1)	98.5(10.1)	( $10^+$ ) $\rightarrow$ ( $9^+$ )
268.6(1)	10.6(1.3)	( $10^+$ ) $\rightarrow$ ( $8^+$ )
284.6(1)	100(10.3)	( $11^+$ ) $\rightarrow$ ( $10^+$ )
291.0(1)	72.4(7.5)	( $12^+$ ) $\rightarrow$ ( $11^+$ )
354.6(1)	41.6 <sup>b</sup> (4.4)	( $14^+$ ) $\rightarrow$ ( $13^+$ )
407.9(1)	37.4(4.0)	( $13^+$ ) $\rightarrow$ ( $12^+$ )
453.4(1)	21.1(2.4)	( $11^+$ ) $\rightarrow$ ( $9^+$ )
575.7(2)	26.1(2.9)	( $12^+$ ) $\rightarrow$ ( $10^+$ )
$\pi [413]_{\frac{5}{2}}^- \otimes \nu h_{11/2}$ band:		
188.6(1)	15.2(1.7)	( $14^-$ ) $\rightarrow$ ( $13^-$ )
211.4(1)	24.5(2.7)	( $15^-$ ) $\rightarrow$ ( $14^-$ )
244.7(1)	28.9(3.1)	( $16^-$ ) $\rightarrow$ ( $15^-$ )
299.8(1)	17.2(2.0)	( $17^-$ ) $\rightarrow$ ( $16^-$ )

<sup>a</sup>The intensity for the delayed transition is shown as a percentage of the total delayed projection, as only one delayed  $\gamma$  ray is observed in this nucleus.

<sup>b</sup>The 355-keV transition could not be separated from the 353-keV transition, and the intensity represents the combined intensity of the two transitions, see Fig. 4.

#### IV. DISCUSSION

The previous high-spin studies of  $^{136}\text{Pm}$  employed thin targets surrounded by a germanium array, with no auxiliary detectors to detect delayed radiation. These experiments were, therefore, not sensitive to  $\gamma$ -ray decays from isomeric states with a half-life greater than a few nanoseconds. The observation of the  $1.5(1) \mu\text{s}$  isomer in this work does not change the established prompt high-spin level scheme of  $^{136}\text{Pm}$ , and the observations of the  $\nu h_{11/2} \otimes \pi h_{11/2}$  yrast transitions built upon the  $J^\pi = (8^+)$  state in this study are entirely in agreement with those in previous works [3,7]. However, the observation of the decay of this  $1.5(1) \mu\text{s}$  isomer gives new information in the region between the well-known high-spin states [3,7] and the low-spin states populated in  $\beta$  decay [11].

To fully characterize this new isomer in  $^{136}\text{Pm}$ , the spins of the states involved in the isomer decay are ideally required. The current experimental setup did not permit angular distribution measurements to be made for these delayed transitions. In addition, because the energy of the new delayed transition (43 keV) falls below the  $K$ -shell binding energy (45.18 keV), the usual  $K$ -shell conversion-coefficient analysis from intensity arguments could not be made to determine the multipolarity of the transition. (It may convert via the  $L$  and higher shells, but the associated x rays would be entirely attenuated by the DSSDs in front of the GREAT HPGe planar.)

Despite this uncertainty in the multipolarity of the 43-keV isomer decay in the  $N = 75$  odd-odd nucleus  $^{136}\text{Pm}$ , information can be gained from the systematics of isomers in the neighboring nuclei where several isomers built upon  $J^\pi = 8^+$  states are known to exist. The  $N = 77$  odd-odd nuclei,  $^{138}_{61}\text{Pm}$  [19],  $^{140}_{63}\text{Eu}$  [20],  $^{142}_{65}\text{Tb}$ , and  $^{144}_{67}\text{Ho}$  [6,20], all have  $J^\pi = 8^+$  isomers decaying by low-energy  $E1$  transitions to  $J^\pi = 7^-$  states (174 keV in  $^{138}\text{Pm}$ , 37 keV and 98 keV in  $^{140}\text{Eu}$ , 37 keV in  $^{142}\text{Tb}$ , and at 56 keV in  $^{144}\text{Ho}$ ). In the  $N = 73$  odd-odd nucleus,  $^{134}_{61}\text{Pm}_{73}$ , a similar yrast band structure has

TABLE II. Weisskopf single-particle half-life estimates for the various possible multiplicities of the 1.5(1)  $\mu$ s delayed 43-keV transition in  $^{136}\text{Pm}$ . The reduced-transition probabilities and associated general recommended upper limits for nuclei in the  $A = 91$ –150 region are also shown [23].

Assumed multipolarity	Weisskopf 43-keV half-life (s)	Reduced-transition probability (W.u.)	Recommended upper limit [23]
$M1$	$1.59 \times 10^{-10}$	$2.8(2) \times 10^{-5}$	1
$M2$	$5.28 \times 10^{-3}$	27(2)	1
$M3$	$2.39 \times 10^5$	$2.6(2) \times 10^7$	10
$E1$	$3.37 \times 10^{-12}$	$1.6(1) \times 10^{-6}$	0.01
$E2$	$9.56 \times 10^{-5}$	1.1(1)	300
$E3$	$4.26 \times 10^3$	$7.7(5) \times 10^5$	100

been assigned; however, this is built upon a  $J^\pi = (7^-)$  state [21]. Recent data from recoil-isomer tagging on this nucleus has revealed that this  $J^\pi = (7^-)$  state is an 18(3)  $\mu$ s isomeric state [22]. The isomer decays by a 71-keV transition whose associated electron conversion is only consistent with  $E1$  multipolarity [22]. The  $N = 75$  odd-odd isotone,  $^{134}\text{Pr}$  [3], shows a similar structure to that of  $^{136}\text{Pm}$ , and comparisons between the two nuclei have already been drawn at higher spins [3]. However, the yrast structure of  $^{134}\text{Pr}$  is only known above the  $J^\pi = (8^+)$  state, and although the lower-lying states are also known from  $\beta$  decay, much like  $^{136}\text{Pm}$ , nothing is known as yet of the intermediate structure.

To decide the most likely multipolarity assignment for the new 1.5(1)  $\mu$ s 43-keV delayed  $\gamma$  ray in  $^{136}\text{Pm}$ , the reduced-transition probabilities,  $t_{1/2}(\text{Weisskopf})/t_{1/2}(\text{experiment})$ , for the isomer decay have been compared with the recommended upper limits for nuclei in the  $A = 91$ –150 region [23]. Table II shows this comparison (corrected for internal conversion) along with the single-particle Weisskopf estimates for the 43-keV delayed transition for various possible decay multiplicities. These Weisskopf estimates show that the

43-keV transition cannot be of  $M2$ ,  $M3$ , or  $E3$  character, as the associated single-particle half-lives are too long and the reduced-transition probabilities exceed the recommended upper limits for  $A = 91$ –150 nuclei by several orders of magnitude. (Although the  $E2$  single-particle Weisskopf half-life estimate is also larger than the experimental value, it is currently not discounted. Its reduced-transition probability remains well within the recommended upper limits, and further consideration of this possible multipolarity is discussed below.) This leaves only the possibilities of  $M1$ ,  $E1$ , or  $E2$  multipolarity for the delayed 43-keV transition in  $^{136}\text{Pm}$ . A more detailed comparison of the experimental reduced-transition probabilities for nuclei in the immediate vicinity of  $^{136}\text{Pm}$  with similar transition energies and initial- and final-level spins is given in Table III from Ref. [23] along with the values for the  $N = 77$  isotones ( $^{138}\text{Pm}$  [19],  $^{140}\text{Eu}$  [20], and  $^{142}\text{Tb}$  and  $^{144}\text{Ho}$  [6,20]).

This comparison of the reduced-transition probabilities for assumed  $E1$ ,  $M1$ , and  $E2$  43-keV decay transitions (Table II) in  $^{136}\text{Pm}$  with the those in the neighboring nuclei (Table III) shows that the most likely multipolarity assignment

 TABLE III. Experimental reduced-transition probabilities for a series of  $E1$ ,  $M1$ , and  $E2$  transitions for nuclei in the vicinity of  $^{136}\text{Pm}$  from Ref. [23].

Nucleus	$E_\gamma$ (keV)	Assigned multipolarity	$J_f^\pi \rightarrow J_i^\pi$	$t_{1/2}$ (ns)	Reduced-transition probability (W.u.)
$^{144}\text{Gd}$	87	$E1$	$10^+ \rightarrow 9^-$	188(14)	$1.7(2) \times 10^{-6}$
$^{148}\text{Dy}$	95	$E1$	$8^+ \rightarrow 7^-$	95(30)	$1.7(6) \times 10^{-6}$
$^{138}\text{Pm}$	174	$E1$	$8^+ \rightarrow 7^-$	21(5)	$2.2(5) \times 10^{-6}$
$^{140}\text{Eu}$	37	$E1$	$8^+ \rightarrow 7^-$	299(3)	$7.6(8) \times 10^{-6}$
$^{140}\text{Eu}$	98	$E1$	$8^+ \rightarrow 7^-$	299(3)	$1.4(1) \times 10^{-7}$
$^{142}\text{Tb}$	37	$E1$	$8^+ \rightarrow 7^-$	$20(1) \times 10^3$	$1.4(1) \times 10^{-7}$
$^{144}\text{Ho}$	57	$E1$	$8^+ \rightarrow 7^-$	519(5)	$1.1(1) \times 10^{-6}$
$^{133}\text{Cs}$	81	$E2$	$7/2^+ \rightarrow 5/2^+$	9.09(3)	5.1(1)
$^{134}\text{Te}$	115	$E2$	$6^{(+)} \rightarrow 4^{(+)}$	237(4)	2.0(1)
$^{135}\text{Te}$	50	$E2$	$(19/2^-) \rightarrow (15/2^-)$	740(30)	3.8(2)
$^{133}\text{La}$	88	$M1$	$(5/2^+) \rightarrow 5/2^+$	1.88(14)	$9.3(7) \times 10^{-3}$
$^{133}\text{Cs}$	81	$M1$	$7/2^+ \rightarrow 5/2^+$	9.09(3)	$2.3(2) \times 10^{-3}$
$^{136}\text{Pr}$	40	$M1$	$(2^+) \rightarrow 2^+$	13.6(3)	$9.4(2) \times 10^{-2}$
$^{136}\text{I}$	87	$M1$	$(2^-) \rightarrow (2^-)$	580(140)	$3.8(9) \times 10^{-3}$

for the new isomer decay is  $E1$ . The reduced-transition probability for this 43-keV  $E1$  transition,  $1.6(1) \times 10^{-6}$ , is consistent with the experimental values for delayed  $E1$  transitions from the  $J^\pi = 8^+$  state in  $^{148}\text{Dy}$ , the  $J^\pi = 10^+$  state in  $^{144}\text{Gd}$ , the  $J^\pi = 8^+$  state in  $^{144}\text{Ho}$ , and the  $J^\pi = 8^+$  state in  $^{138}\text{Pm}$ . The agreement with the other known  $J^\pi = 8^+$  states in  $^{142}\text{Tb}$ ,  $^{140}\text{Eu}$  (98 keV), and  $^{140}\text{Eu}$  (37 keV) is poorer, being factors of 11, 11, and 0.2 times too large. The comparison for the alternative  $M1$  [ $2.8(2) \times 10^{-5}$  W.u.] and  $E2$  [1.1(1) W.u.] assignments shows no consistency at all with other known  $M1$  and  $E2$  decays [23]. However, because the reduced-transition probabilities for these  $M1$  and  $E2$  alternative assignments still fall below the recommended upper limits discussed in Ref. [23] and Table II above, they cannot be fully dismissed.

To understand the reasons for the long half-life for this  $J^\pi = (8^+)$  state in  $^{136}\text{Pm}$ , total Routhian surface (TRS) calculations [24] have been performed. At zero rotational frequency, these calculations predict that  $^{136}\text{Pm}$  has deformation parameters given by  $(\beta_2, \beta_4, \gamma) = (0.21, -0.02, -23^\circ)$ . The predicted quadrupole deformation parameter  $\beta_2 = 0.21$  compares well with that from Möller and Nix,  $\beta_2 = 0.22$  [25], which does not, however, include nonaxial behavior. (These parameters remain valid in the TRS calculations up to higher rotational frequencies: at  $\hbar\omega = 0.201$  MeV,  $\beta_2$  and  $\beta_4$  remain the same while  $\gamma$  increases in magnitude to  $-28^\circ$ .) Using  $\beta_2 = 0.21$  with the Nilsson model, the configuration of possible states can be postulated for this nonrotational intrinsic  $J^\pi = (8^+)$  isomeric bandhead state. Assuming for the bandhead,  $K = I$ , then the most likely configuration for the  $J^\pi = (8^+)$  state is  $\nu h_{11/2}[505]_{\frac{11}{2}}^- \otimes \pi h_{11/2}[532]_{\frac{5}{2}}^-$ . This configuration may be expected to have a triaxial shape, since the neutron  $h_{11/2}[505]_{\frac{11}{2}}^-$  orbit strongly favors an oblate shape while the proton  $h_{11/2}[532]_{\frac{5}{2}}^-$  orbit strongly favors a prolate shape. For a deformation of  $\beta_2 = 0.21$ , the state below would be the  $J^\pi = (7^-)$ ,  $\nu h_{11/2}[505]_{\frac{11}{2}}^- \otimes \pi d_{5/2}[411]_{\frac{3}{2}}^+$  state. This configuration may be expected to strongly favor an oblate shape, as the  $h_{11/2}[505]_{\frac{11}{2}}^-$  neutron is strongly oblate driving and the proton  $d_{5/2}[411]_{\frac{3}{2}}^+$  orbit has no shape preference. This shape difference between the  $J^\pi = (8^+)$  and  $J^\pi = (7^-)$

states is likely to be the contributing factor leading to the 1.5(1)  $\mu\text{s}$  lifetime of the new  $J^\pi = (8^+)$  isomeric state observed in  $^{136}\text{Pm}$ .

## V. CONCLUSIONS

In conclusion, the  $(8^+)$  bandhead of the  $\pi h_{11/2} \otimes \nu h_{11/2}$  band in the doubly odd nucleus  $^{136}\text{Pm}$  has been measured for the first time to have a 1.5(1)  $\mu\text{s}$  half-life, using recoil-isomer tagging. The isomer lies below the already established yrast transitions and is depopulated by a delayed 43-keV  $\gamma$ -ray transition. Consideration of the single-particle Weiskopf estimates, reduced-transition probabilities, and their recommended upper limits for isomers in the mass 130 region reveals that the most likely assignment for the 43-keV  $\gamma$ -ray decay from the  $J^\pi = (8^+)$  isomeric state is an  $E1$  transition. The Nilsson model predicts that the  $J^\pi = (8^+)$  isomeric state is built upon the  $\nu h_{11/2}[505]_{\frac{11}{2}}^- \otimes \pi h_{11/2}[532]_{\frac{5}{2}}^-$  orbits, and the  $J^\pi = (7^-)$  state on the  $\nu h_{11/2}[505]_{\frac{11}{2}}^- \otimes \pi d_{5/2}[411]_{\frac{3}{2}}^+$  orbits. The long lifetime of the isomeric state is reasoned to be due to the differing shape-driving effects of the  $J^\pi = (8^+)$  and  $J^\pi = (7^-)$  configurations. In the present work, no prompt or delayed  $\gamma$ -ray coincidences were found to link the new  $J^\pi = (7^-)$  state to the lower-spin long-lived  $J^\pi = (5^-)$  and  $(2^+)$  states observed in the  $\beta$ -decay work [11]. This may suggest that the newly observed  $J^\pi = (7^-)$  state may feed another, longer-lived, isomeric state with a half-life of the order of milliseconds or greater. Alternatively, this longer-lived state may not decay by emission of  $\gamma$  rays, but by  $\beta$  decay or internal conversion.

## ACKNOWLEDGMENTS

This work has been supported by the EU Sixth Framework Programme, “Integrating Infrastructure Initiative-Transnational Access,” Contract No. 506065 (EURONS) and by the Academy of Finland under the Finnish Centre of Excellence Programme 2006–2011 (Nuclear and Accelerator Based Physics Programme at JYFL). SVR, PJRM, and DTS also acknowledge receipt of EPSRC grants.

- 
- [1] I. Ragnarsson *et al.*, Nucl. Phys. **A233**, 329 (1974).  
 [2] Y. S. Chen, S. Frauendorf, and G. A. Leander, Phys. Rev. C **28**, 2437 (1983).  
 [3] C. W. Beausang, L. Hildingsson, E. S. Paul, W. F. Piel Jr., N. Xu, and D. B. Fossan, Phys. Rev. C **36**, 1810 (1987) and references therein.  
 [4] K. Starosta *et al.*, Phys. Rev. Lett. **86**, 6, 971 (2001).  
 [5] D. M. Cullen *et al.*, Phys. Rev. C **66**, 034308 (2002).  
 [6] C. Scholey *et al.*, Phys. Rev. C **63**, 034321 (2001).  
 [7] M. A. Riley *et al.*, Phys. Rev. C **47**, R441 (1993).  
 [8] J. Pfohl *et al.*, Phys. Rev. C **62**, 031304(R) (2000).  
 [9] A. A. Hecht *et al.*, Phys. Rev. C **63**, 051302(R) (2001).  
 [10] D. J. Hartley *et al.*, Phys. Rev. C **64**, 031304(R) (2001).  
 [11] K. S. Vierinen, J. M. Nitschke, P. A. Wilmarth, R. B. Firestone, and J. Gilat, Nucl. Phys. **A499**, 1 (1989).  
 [12] M. Leino *et al.*, Nucl. Instrum. Methods Phys. Res. B **99**, 653 (1995).  
 [13] R. D. Page *et al.*, Nucl. Instrum. Methods Phys. Res. B **204**, 634 (2003).  
 [14] P. Rakhila, Nucl. Instrum. Methods Phys. Res. A (2008).  
 [15] I. Lazarus *et al.*, IEEE Trans. Nucl. Sci **48**, 567 (2001).  
 [16] D. M. Cullen *et al.*, Phys. Rev. C **58**, 846 (1998).  
 [17] W. T. Milner, “UPAK, the Oak Ridge Analysis Package” in the Holifield Heavy Ion Research Facility Computer Handbook (Oak Ridge National Laboratory, Tennessee, 1987).  
 [18] D. Bazzacco *et al.*, Phys. Rev. C **58**, 2002 (1998).  
 [19] C. W. Beausang, P. K. Wang, R. Ma, E. S. Paul, W. F. Piel Jr., N. Xu, and D. B. Fossan, Phys. Rev. C **42**, 541 (1990).

- [20] M. N. Tantawy *et al.*, Phys. Rev. C **73**, 024316 (2006).
- [21] R. Wadsworth, S. M. Mullins, P. J. Bishop, A. Kirwan, M. J. Godfrey, P. J. Nolan, and P. H. Regan, Nucl. Phys. **A526**, 188 (1991).
- [22] P. J. R. Mason *et al.* (private communication).
- [23] P. M. Endt, At. Data Nucl. Data Tables **26**, 41 (1981).
- [24] W. Nazarewicz, R. Wyss, and A. Johnson, Nucl. Phys. **A503**, 285 (1989).
- [25] P. Möller, J. R. Nix, W. D. Myers, and W. J. Swiatecki, At. Data Nucl. Data Tables **59**, 185 (1995).